# The nearly classical behavior of a pure fluid on the critical isochore very near the critical point under the influence of gravity[1]

N. Kurzeja[2], Th. Tielkes[2], and W. Wagner[2,3]

---

[1] Paper presented at the Thirteenth Symposium on Thermophysical Properties, June 22-27, 1997, Boulder, Colorado, U.S.A.

[2] Lehrstuhl für Thermodynamik, Ruhr-Universität Bochum, D-44780 Bochum, Germany.

[3] To whom correspondence should be addressed.

**ABSTRACT**

Comprehensive measurements of the isothermal compressibility along the critical isochore in the critical region of pure sulfurhexafluoride ($SF_6$) and pure carbon dioxide ($CO_2$) were carried out. All the measurements were performed with a multi-cell apparatus, especially designed for $p\rho T$ measurements in the critical region. The height of the measuring cells was either 30 mm or 11 mm. Regardless of the cell height we have found for both fluids nearly "classical" values for the critical exponent $\gamma$ in the limiting approach to the critical point. However, at a certain distance from the critical point $\{(T-T_c) \approx 85$ mK or $\tau \approx 2.7\cdot10^{-4}$ for $SF_6$ and $(T-T_c) \approx 55$ mK or $\tau \approx 1.8\cdot10^{-4}$ for $CO_2\}$ we observed a transition to values of the critical exponents which nearly meet the predictions of the renormalization-group theory. We conclude that the reason for the different behavior is an explicit gravity effect governing the inner critical region. The two different loci of the transition points for sulfurhexafluoride and carbon dioxide can be attributed to the different gravity impact on the fluid corresponding to the different critical densities of the two substances.

KEY WORDS: carbon dioxide, critical exponent, critical point, differential pressure, gravity, isothermal compressibility, multi-cell apparatus, sulfurhexafluoride.

## 1. INTRODUCTION

In order to measure the thermal behavior in the critical region of pure fluids considerably more accurately than it had been possible before, a new special $p\rho T$ multi-cell apparatus was developed [1, 2]. In 1990, we finished our first $p\rho T$ measurements in the critical region of sulfurhexafluoride ($SF_6$), which had been the first comprehensive direct $p\rho T$ measurements in the really near-critical region. The results of these measurements were reported at the 11th Symposium on Thermophysical Properties [3]. In the limiting approach to the critical point we found nearly classical values for the critical exponents $\beta$, $\gamma$, and $\delta$. However, at a certain distance from the critical point we observed a transition to non-classical behavior as predicted by the renormalization-group theory. Based on the corrections for density stratification, this transition point could be identified as the limit of gravity influence on the thermal behavior of $SF_6$. For a better clarification of these surprising results we therefore carried out more experiments which focused on the influence of gravity.

In a first step we used new "horizontal" measuring cells with a height of only 11 mm in addition to the 30 mm high cells. With these new cells we repeated our previous [3] measurements of the isothermal compressibility on the critical isochore of $SF_6$ and found nearly identical results for $\gamma$ [4].

In a second step we varied the fluid itself and performed comprehensive $p\rho T$ measurements in the critical region of carbon dioxide ($CO_2$) and studied again the isothermal compressibility along the critical isochore. For both a cell height of 30 mm and of 11 mm the new results for $CO_2$ are in remarkable agreement with the results obtained for $SF_6$. A detailed description of these measurements is given in separate papers [5-8].

In this paper we concentrate only on all the measurements of the isothermal compressibility which we performed along the critical isochore, both on $SF_6$ and on $CO_2$.

## 2. EXPERIMENTAL

The measuring principle and the design of the multi-cell apparatus with its four-stage high-precision thermostat has already been described in a previous paper [3]. The reason for creating this special $p\rho T$ multi-cell apparatus was to attain an extremely high internal

consistency of the single $p\rho T$ measuring points with regard to temperature, pressure, and density. For this reason not only one single measuring cell but a whole block of measuring cells is built into a high-precision thermostat. The isothermal pressure differences between the cells filled with fluid of different density are directly measured with high-precision differential pressure indicators (DPI). For measurements of the isothermal compressibility the two arrangements of measuring cells, as shown in Fig. 1, were used.

In order to vary the height of the measuring cells the differential pressure indicator is either horizontally or vertically aligned. In the latter case the cell height is given by the diameter of the membranes of the DPI. The DPIs are directly flanged to the cells via metal-lip seals developed by ourselves. Not shown in Fig. 1 are the all-metal valves also directly integrated in the measuring cell. We designed two different blocks of measuring cells composed of either vertical or vertical and horizontal cells. Both blocks fit within our high-precision thermostat and meet the extreme requirements for the temperature gradients given by the isothermal principle of measuring isothermal compressibilities. The temperature stability with regard to time is better than ±10 μK (over hours) and ±25 μK (over days), respectively. As verified by several measurements (exchanging the places of 25 Ω platinum thermometers) the temperature gradient over the entire block of measuring cells is smaller than ±35 μK; therefore, over a single cell the gradient can be estimated to be smaller than ±10 μK. For measuring and controlling the absolute temperature we use 25 Ω platinum resistance thermometers and AC resistance bridges. In this way we achieved a consistency of the temperature measurements of better than ±25 μK and an uncertainty in the absolute temperature of less than ±1 mK.

The process of filling the measuring cells with the fluid of desired density is based on $p\rho T$ data measured by Gilgen et al. [9] for $SF_6$ and by Nowak et al. [10] for $CO_2$. When taking into account the uncertainty of the filled-in densities, the change in cell volume due to time, temperature, pressure and displacement of the membranes of the differential pressure indicators, the Gaussian error-propagation leads to an uncertainty of the actual density within the measuring cells of $\Delta\rho/\rho \leq \pm 5\cdot 10^{-4}$.

The total uncertainty of the determined differential pressure is based on three influences: the uncertainty of the differential pressure indicators, the uncertainty of the calibration, and the averaging error (see [3, 5]). The uncertainty of the DPIs was minimized by a special mathematical model to take into account the influences of temperature, absolute pressure, and time. A newly developed differential pressure standard ($\Delta(\Delta p) \leq \pm 2$ Pa) was used for a careful calibration of the DPIs. The averaging error was corrected by computing the density stratification with convenient equations of state. In this way for the differential pressure measured between two cells we obtained a consistency of better than ±0.2 Pa and an uncertainty of $\Delta(\Delta p) \leq \pm 6$ Pa.

With these consistencies and accuracies in the measured values of temperature, differential pressure and density it was possible to determine very consistent and precise values of the isothermal compressibility along the critical isochore. For this purpose a set of either two vertical or two horizontal measuring cells (see Fig. 1) was filled "symmetrically around the critical density", which means that the fluid density in one of the two cells was slightly above the critical density and in the other cell the density was slightly below the critical density. The isothermal compressibility $K_T$ is then obtained by the relation

$$K_T = \frac{1}{\rho}\left(\frac{\partial \rho}{\partial p}\right)_T \approx \frac{1}{\rho}\left(\frac{\Delta \rho}{\Delta p}\right)_T \quad , \tag{1}$$

where $\rho$ is the averaged density of the two cells and $\Delta\rho$ and $\Delta p$ are the differences in density and pressure, respectively, between the two cells; $\Delta p$ is directly measured with the DPI.

The sulfurhexafluoride used for the measurements was supplied by Air Products, Germany, and purified by ourselves. Analyses performed by Linde, Germany, before and after the measurements did not yield any detectable impurities $\{x(N_2) \leq 1\cdot10^{-6}$; $x(O_2) \leq 1\cdot10^{-6}$; $x(CF_4) \leq 1\cdot10^{-6}$; $x(He) \leq 0.5\cdot10^{-6}$; $x(H_2O) \leq 1\cdot10^{-6}$; $x(\text{hydrocarbons}) \leq 1\cdot10^{-6}$ where $x$ denotes mole fraction$\}$. We expect the achieved purity to be $x(SF_6) \geq 0.999994$. The carbon dioxide was supplied by Messer Griesheim, Germany, with a certified purity of $x(CO_2) \geq 0.999999$. Again, the fluid was analyzed before and after the measurements by Messer Griesheim and no detectable impurities were found $\{x(N_2) \leq 0.2\cdot10^{-6}$; $x(O_2) \leq 0.2\cdot10^{-6}$; $x(CO) \leq 0.01\cdot10^{-6}$; $x(He) \leq 0.5\cdot10^{-6}$; $x(H_2O) \leq 0.3\cdot10^{-6}$; $x(\text{hydrocarbons}) \leq 0.01\cdot10^{-6}\}$.

## 3. RESULTS

The critical exponent $\gamma$ is defined through the power law

$$K_T = \Gamma \cdot \left( \frac{T - T_c}{T_c} \right)^{-\gamma} \tag{2}$$

and can be determined by nonlinear fitting of the parameters $\Gamma$, $T_c$ and $\gamma$ to the experimental values of the isothermal compressibility $K_T$ along the critical isochore. In the fitting process it turned out that there are two different regions for which Eq. (2) yields systematically different values for $\gamma$. As shown in Figs. 2 to 5 we found for both fluids, carbon dioxide and sulfurhexafluoride, and for both types of measuring cells, vertical and horizontal ones, an inner region, where the determined parameter $\gamma$ in Eq. (2) becomes about 1.0. The data points in the last few mK close to $T_c$ had to be kept out of the fit due to the sharp increase of their uncertainty ($K_T$ goes to infinity). Beyond a more or less distinct transition point $\{(T - T_c) \approx 85$ mK or $\tau \approx 2.7 \cdot 10^{-4}$ for $SF_6$ and $(T - T_c) \approx 55$ mK or $\tau \approx 1.8 \cdot 10^{-4}$ for $CO_2\}$, for the outer region the fit yields a value for $\gamma$ of about 1.2. It should be noted clearly that any attempt to fit Eq. (2) simultaneously to $K_T$ data points from the inner and outer temperature region leads to a systematic misrepresentation of the experimental data.

We observed these surprising different regions for all of our measurements. An overview of the various experimental runs carried out with $SF_6$ ($\rho_c = 742.15$ kg·m$^{-3}$) and $CO_2$ ($\rho_c = 467.6$ kg·m$^{-3}$) is given in Tables I to IV. In Tables II and IV, the values listed for the fitted parameters $\gamma$ and $T_c$ in Eq. (2) are referred to as $\gamma_f$ and $T_{c,f}$. They were determined from $K_T$ data measured in an outer, "far-critical" region; these values do not represent the critical parameter $\gamma$ and the critical temperature $T_c$. Experimental values for $\gamma$ and $T_c$ are reported in Tables I and III. Strong evidence that the inner region is the "right" one, which suits the power law within its physical meaning, is given by the values of critical temperature. Thus, the values for $T_c$ obtained from fitting Eq. (2) to data from the inner region are in excellent agreement ($\Delta T_c \leq \pm 1$ mK) with the critical temperature which we determined with an independent method as $T_c = 318.7232$ K $\pm 2$ mK for $SF_6$ and $T_c = 304.1363$ K $\pm 2$ mK for $CO_2$ (see [5-8]).

As reported in [3, 5, 6] we developed a mathematical model to correct the averaging

error due to the gravity-induced density stratification in the measuring cells (implicit gravity effect). This implies the use of an equation of state that represents the experimental data nearly within their consistency. For carrying out these corrections we have developed analytical equations of state for the critical region of $SF_6$ and $CO_2$ which meet this requirement. Alternatively, we have also used revised and extended scaling equations for such corrections. Although this type of equations does not represent our data properly, the determined values for the critical exponent $g$ are in the range between 0.92 and 1.10. These tests show clearly that the type of equation of state used for these corrections is definitely not responsible for our almost classical values for $g$, which we state as:

$$g = 0.98 \pm 0.04 \quad \text{for } SF_6, \tag{3}$$

$$g = 0.99 \pm 0.04 \quad \text{for } CO_2. \tag{4}$$

When determining the parameter $g_f$ of the outer region ($g_f = 1.20 \pm 0.03$ for $SF_6$, respectively $g_f = 1.20 \pm 0.04$ for $CO_2$) the equation of state has no impact, since here the influence of the averaging error decreases clearly. We emphasize that for the inner region the averaging error and its correction for horizontal and vertical cells differ in type and size. Consequently, we exclude an error in the mathematical model or in computation which is significant for the considerations given above.

The new results are in clear contradiction to the predictions of the renormalization-group theory and to most experimental results reported by other authors [11-16]. However, our measurements were performed with the smallest temperature gradients and the highest purity of fluid ever reported. More than this, in contrast to optical experiments our experimental $K_T$ values are *directly* based on measured differential pressures and densities according to Eq. (1), and do not depend on the Lorentz-Lorenz relation which is unproven in the gravity influenced critical region. Notably, there is a certain agreement when comparing our results with the experiments of Makarevich et al. [17] and Ivanov [18], who performed direct measurements with extremely pure $SF_6$ and also found two regions of different fluid behavior.

On account of our results we believe that in the immediate vicinity of the critical point

pure fluids under gravity show a universal but nearly classical-like behavior. Apparently in this region the fluid behavior is governed by an explicit gravity effect, which was not expected to be so strong (see [19-20]). In an outer region where gravity-induced density stratification plays no part, fluid behavior is approximately described by the renormalization-group theory. The change between the two different kinds of universal fluid behavior occurs at a transition point which seems to depend on the gravity impact on the fluid as indicated by the relation $t_{trans.point}(CO_2)/t_{trans.point}(SF_6) \approx r_c(CO_2)/r_c(SF_6) \approx 2/3$.

**ACKNOWLEDGMENTS**

The authors acknowledge the assistance given by all who contributed to this work, especially B. Pieperbeck for performing a part of the measurements and P. Claus and H.-J. Collmann for carrying out parts of the computational work. Above all, the authors thank the Deutsche Agentur für Raumfahrtangelegenheiten GmbH (DARA) for financial support of this work under Grant 50 QV 9052.

## REFERENCES


1. H.-G. Kratz, and W. Wagner, *Meßapparatur zur Druck-, Dichte-, Temperatur-(p,v,T)-Messung im kritischen Gebiet reiner fluider Stoffe*. Forsch.-Ber. BMFT W 85-006 (BMFT, Bonn, 1985).
2. N. Kurzeja, *Entwicklung und Aufbau einer Meßapparatur nach der pρT-Mehrzellen-methode zur Messung des thermischen Zustandsverhaltens im kritischen Gebiet reiner fluider Stoffe*. Dissertation Ruhr-Universität Bochum (Bochum, 1990).
3. W. Wagner, N. Kurzeja, and B. Pieperbeck, *Fluid Phase Equilibria* **79**: 151 (1992).
4. W. Wagner, N. Kurzeja, and Th. Tielkes, in *Abstracts of the Ninth European Symposium of Gravity-Dependent Phenomena in Physical Sciences* (Berlin, 1995), pp. 81-82.
5. Th. Tielkes, N. Kurzeja, and W. Wagner, *Präzisionsmessungen der thermischen Zustandsgrößen im kritischen Gebiet von Kohlendioxid*. Fortschr.-Ber. VDI, R 3, Nr. 488 (VDI-Verlag, Düsseldorf, 1997).
6. Th. Tielkes, N. Kurzeja, and W. Wagner, *The thermal behavior of carbon dioxide in the critical region - results from recent pρT measurements with a multi-cell apparatus.* To be submitted to the Int. J. Thermophys.
7. Th. Tielkes, N. Kurzeja, and W. Wagner, *Reference data for the critical region of carbon dioxide - results from recent pρT measurements with a multi-cell apparatus.* To be submitted to the Int. J. Thermophys.
8. N. Kurzeja, Th. Tielkes, and W. Wagner, *The p-T relation along the critical isochore in the critical region of sulfurhexafluoride and carbon dioxide*. To be submitted to the Int. J. Thermophys.
9. R. Gilgen, R. Kleinrahm, and W. Wagner, *J. Chem. Thermodyn.* **24**: 1243 (1992).
10. P. Nowak, Th. Tielkes, R. Kleinrahm, and W. Wagner, accepted for publication in *J. Chem. Thermodyn.* **29** (1997).
11. G. T. Feke, G. A. Hawkins, J. B. Lastovka, and G. B. Benedek, *Phys. Rev. Lett.* **27**: 1780 (1971).
12. D. A. Balzarini, *Can. J. Phys.* **50**: 2194 (1972).
13. D. S. Canell, *Phys. Rev. A* **12**: 225 (1975).
14. R. Hocken, and M. R. Moldover, *Phys. Rev. Lett.* **37**: 29 (1976).
15. K. Morofuji, K. Fuji, M. Uematsu, and K. Watanabe, *Int. J. Thermophys.* **7**: 17 (1986).
16. J. H. Lunacek, and D. S. Canell, *Phys. Rev. Lett.* **13**: 841 (1971).
17. L. A. Makarevich, O. N. Sokolova, and A. M. Rozen, *Sov. Phys.-JETP* **40**: 305 (1974).
18. D. Y. Ivanov, in *Proceedings of the Eleventh Int. AIRPAT Conference*, Vol. 2 (Le Creusot, 1979), pp. 713-714.
19. J. V. Sengers, and J. M. J. van Leeuwen, *Physica A* **116**: 345 (1982).
20. J. V. Sengers, and J. M. J. van Leeuwen, *Int. J. Thermophys.* **6**: 545 (1985).

Table I. Fitting of Eq. (2) to the Experimental $K_T$ Data for Sulfurhexafluoride (Inner Region).

| Run | Cells | r / (kg·m$^{-3}$) | Δr / (kg·m$^{-3}$) | Temperature range | Data points | $T_c$ / K | g |
|---|---|---|---|---|---|---|---|
| 1 | hor. | 742.06 | 3.33 | 10 mK < ($T$ – $T_c$) < 75 mK | 31 | 318.7223 | 0.956 |
| 2 | vert. | 744.98 | 4.99 | 5 mK < ($T$ – $T_c$) < 84 mK | 51 | 318.7224 | 0.978 |
| 3 | vert. | 739.97 | 5.03 | 6 mK < ($T$ – $T_c$) < 75 mK | 45 | 318.7222 | 0.964 |
| 4 | vert. | 745.46 | 3.09 | 5 mK < ($T$ – $T_c$) < 85 mK | 17 | 318.7225 | 0.993 |
| 5 | vert. | 742.50 | 2.82 | 3 mK < ($T$ – $T_c$) < 85 mK | 18 | 318.7230 | 0.957 |
| 6 | vert. | 744.40 | 14.49 | 5 mK < ($T$ – $T_c$) < 65 mK | 11 | 318.7227 | 0.996 |

Table II. Fitting of Eq. (2) to the Experimental $K_T$ Data for Sulfurhexafluoride (Outer Region).

| Run | Cells | r / (kg·m$^{-3}$) | Δr / (kg·m$^{-3}$) | Temperature range | Data points | $T_{c,f}$ / K | $g_f$ |
|---|---|---|---|---|---|---|---|
| 1 | hor. | 742.06 | 3.33 | 95 mK < ($T$ – $T_c$) < 215 mK | 17 | 318.7045 | 1.202 |
| 2 | vert. | 744.98 | 4.99 | 95 mK < ($T$ – $T_c$) < 215 mK | 30 | 318.7047 | 1.203 |
| 3 | vert. | 739.97 | 5.03 | 101 mK < ($T$ – $T_c$) < 215 mK | 28 | 318.7072 | 1.188 |
| 4 | vert. | 745.46 | 3.09 | 95 mK < ($T$ – $T_c$) < 315 mK | 7 | 318.7011 | 1.216 |
| 5 | vert. | 742.50 | 2.82 | 95 mK < ($T$ – $T_c$) < 315 mK | 7 | 318.6938 | 1.215 |
| 6 | vert. | 744.40 | 14.49 | 65 mK < ($T$ – $T_c$) < 415 mK | 4 | 318.7065 | 1.200 |

Table III. Fitting of Eq. (2) to the Experimental $K_T$ Data for Carbon Dioxide (Inner Region).

| Run | Cells | r / (kg·m$^{-3}$) | Δr / (kg·m$^{-3}$) | Temperature range | Data points | $T_c$ / K | g |
|---|---|---|---|---|---|---|---|
| 1 | hor. | 467.56 | 1.92 | 14 mK < ($T$ – $T_c$) < 52 mK | 22 | 304.1362 | 0.992 |
| 2 | hor. | 467.56 | 1.92 | 14 mK < ($T$ – $T_c$) < 54 mK | 19 | 304.1364 | 0.994 |
| 3 | vert. | 468.51 | 1.99 | 14 mK < ($T$ – $T_c$) < 59 mK | 24 | 304.1363 | 0.994 |
| 4 | vert. | 468.51 | 1.99 | 14 mK < ($T$ – $T_c$) < 59 mK | 22 | 304.1362 | 0.998 |
| 5 | vert. | 467.72 | 2.31 | 19 mK < ($T$ – $T_c$) < 64 mK | 9 | 304.1362 | 0.986 |

Table IV. Fitting of Eq. (2) to the Experimental $K_T$ Data for Carbon Dioxide (Outer Region).

| Run | Cells | r / (kg·m$^{-3}$) | Δr / (kg·m$^{-3}$) | Temperature range | Data points | $T_{c,f}$ / K | $g_f$ |
|---|---|---|---|---|---|---|---|
| 1 | hor. | 467.56 | 1.92 | 54 mK < ($T$ – $T_c$) < 214 mK | 51 | 304.1316 | 1.199 |
| 2 | hor. | 467.56 | 1.92 | 54 mK < ($T$ – $T_c$) < 214 mK | 47 | 304.1296 | 1.194 |
| 3 | vert. | 468.51 | 1.99 | 59 mK < ($T$ – $T_c$) < 214 mK | 49 | 304.1266 | 1.204 |
| 4 | vert. | 468.51 | 1.99 | 49 mK < ($T$ – $T_c$) < 214 mK | 50 | 304.1282 | 1.198 |
| 5 | vert. | 467.72 | 2.31 | 54 mK < ($T$ – $T_c$) < 214 mK | 22 | 304.1266 | 1.207 |

## FIGURE CAPTIONS

Fig. 1. Schematic design of a set of horizontal and a set of vertical measuring cells with directly flanged differential pressure indicator (DPI).

Fig. 2. Percentage deviations of experimental $K_{T,\,\mathrm{expt}}$ values for sulfurhexafluoride (Run 1, horizontal cells) from values $K_{T,\,\mathrm{calc}}$ calculated from Eq. (2) fitted to $K_{T,\,\mathrm{expt}}$ values of the inner temperature range 10 mK < $(T - T_c)$ < 75 mK (upper diagram) and to $K_{T,\,\mathrm{expt}}$ values of the outer temperature range 95 mK < $(T - T_c)$ < 215 mK (lower diagram). The dotted region illustrates the fitting range of the corresponding $K_T$ equation.

Fig. 3. Percentage deviations of experimental $K_{T,\,\mathrm{expt}}$ values for sulfurhexafluoride (Run 2, vertical cells) from values $K_{T,\,\mathrm{calc}}$ calculated from Eq. (2) fitted to $K_{T,\,\mathrm{expt}}$ values of the inner temperature range 5 mK < $(T - T_c)$ < 84 mK (upper diagram) and to $K_{T,\,\mathrm{expt}}$ values of the outer temperature range 95 mK < $(T - T_c)$ < 215 mK (lower diagram). The dotted region illustrates the fitting range of the corresponding $K_T$ equation.

Fig. 4. Percentage deviations of experimental $K_{T,\,\mathrm{expt}}$ values for carbon dioxide (Run 1, horizontal cells) from values $K_{T,\,\mathrm{calc}}$ calculated from Eq. (2) fitted to $K_{T,\,\mathrm{expt}}$ values of the inner temperature range 14 mK < $(T - T_c)$ < 52 mK (upper diagram) and to $K_{T,\,\mathrm{expt}}$ values of the outer temperature range 54 mK < $(T - T_c)$ < 214 mK (lower diagram). The dotted region illustrates the fitting range of the corresponding $K_T$ equation.

Fig. 5. Percentage deviations of experimental $K_{T,\,\mathrm{expt}}$ values for carbon dioxide (Run 3, vertical cells) from values $K_{T,\,\mathrm{calc}}$ calculated from Eq. (2) fitted to $K_{T,\,\mathrm{expt}}$ values of the inner temperature range 14 mK < $(T - T_c)$ < 59 mK (upper diagram) and to $K_{T,\,\mathrm{expt}}$ values of the outer temperature range 59 mK < $(T - T_c)$ < 214 mK (lower diagram). The dotted region illustrates the fitting range of the corresponding $K_T$ equation.

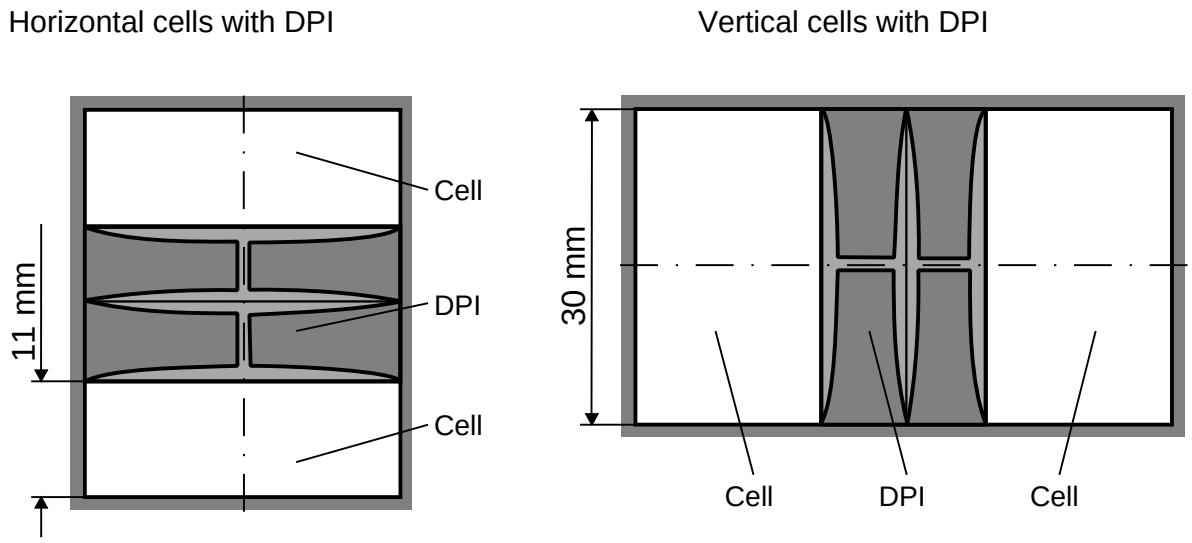
Horizontal cells with DPI
Vertical cells with DPI
Cell
DPI
Cell
11 mm
30 mm
Cell
DPI
Cell

Fig. 1

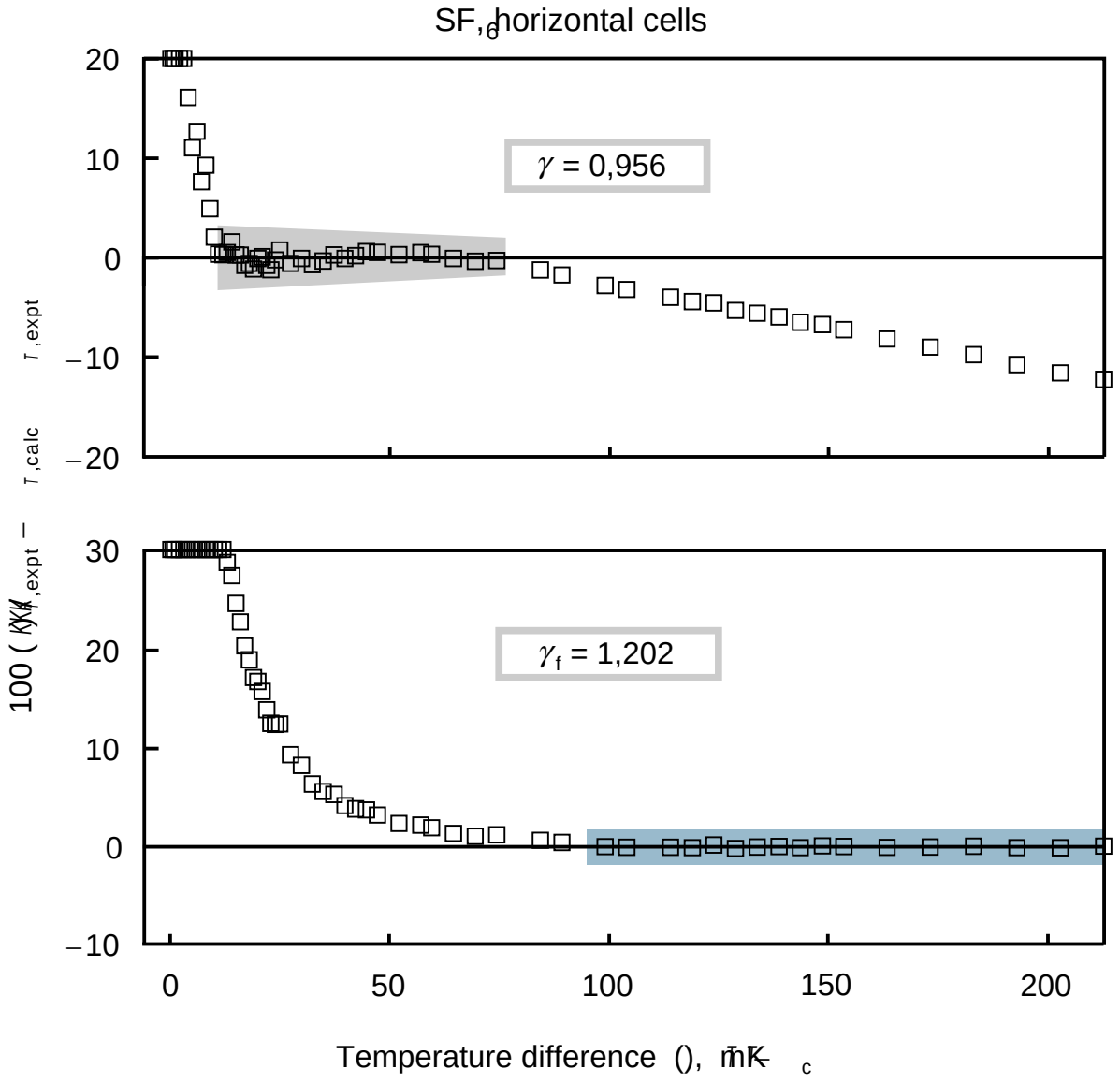
SF6, horizontal cells
20
10
0
−10
−20
γ = 0,956
30
20
10
0
−10
γf = 1,202
0
50
100
150
200
Temperature difference (), mK

Fig. 2

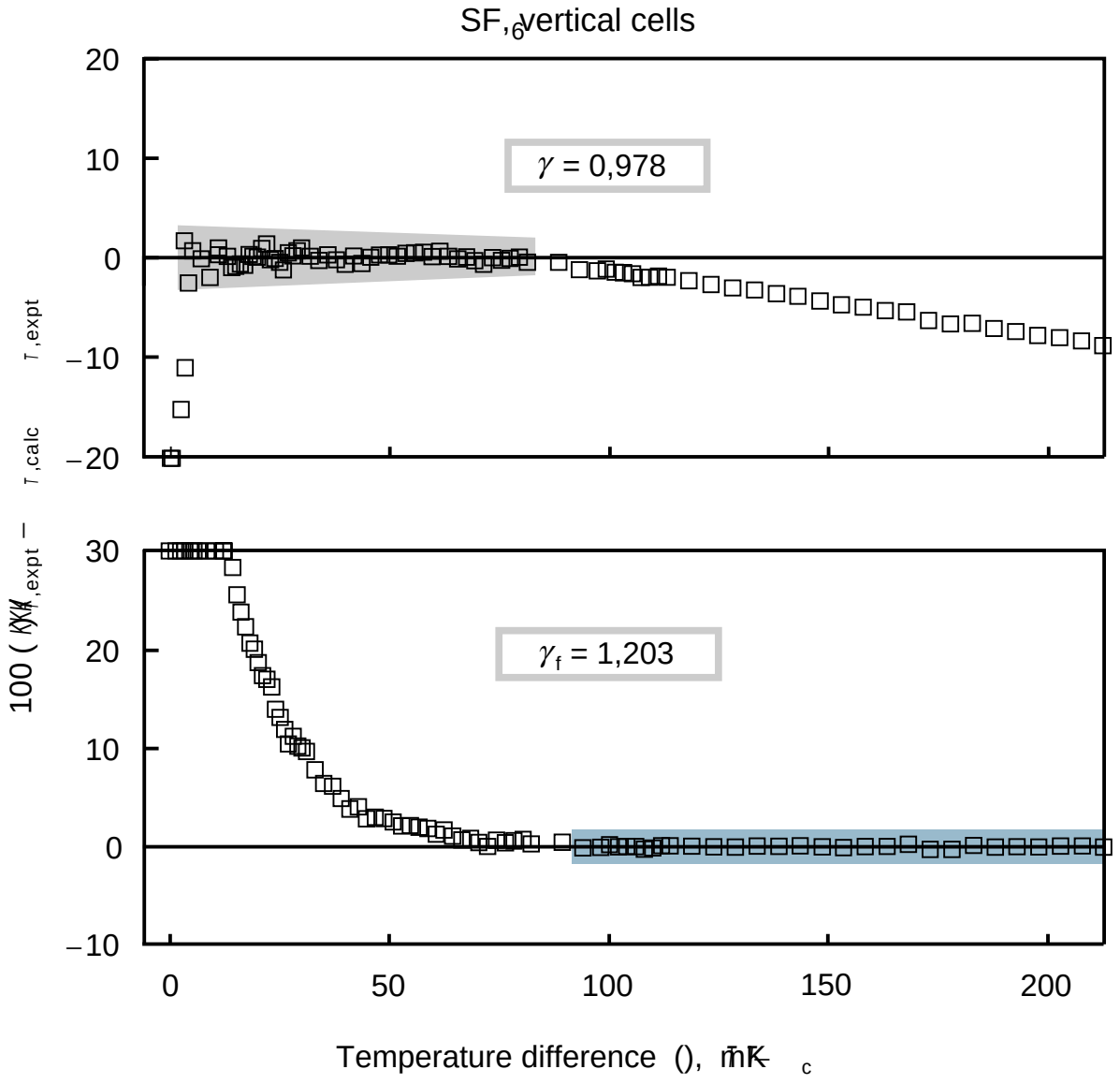
SF6, vertical cells
γ = 0,978
γf = 1,203
20
10
0
−10
−20
30
20
10
0
−10
0
50
100
150
200
Temperature difference (), mK
100 ( )

Fig. 3

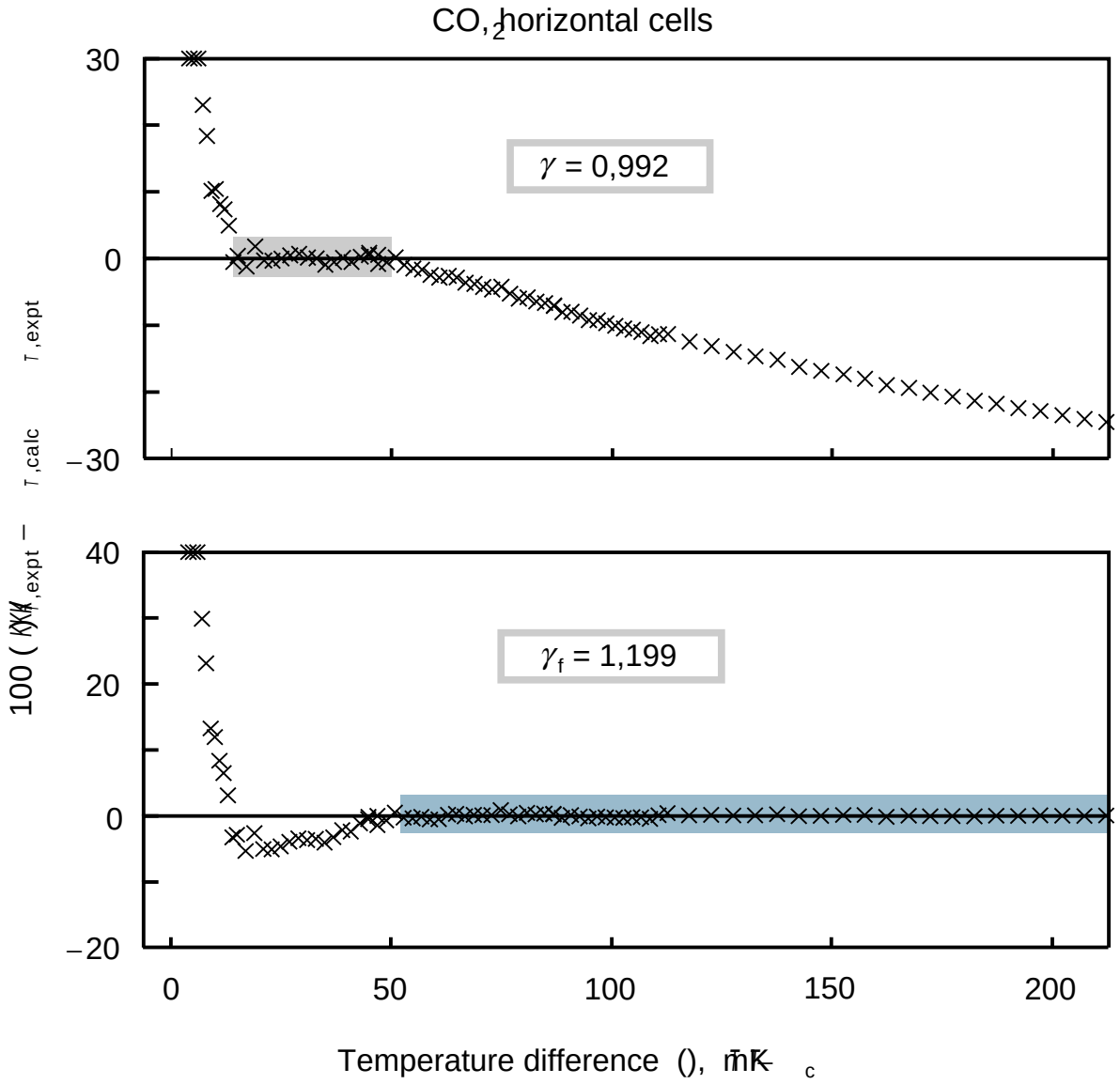
CO2, horizontal cells
30
0
−30
γ = 0,992
40
20
0
−20
γf = 1,199
0
50
100
150
200
Temperature difference (), mK

Fig. 4

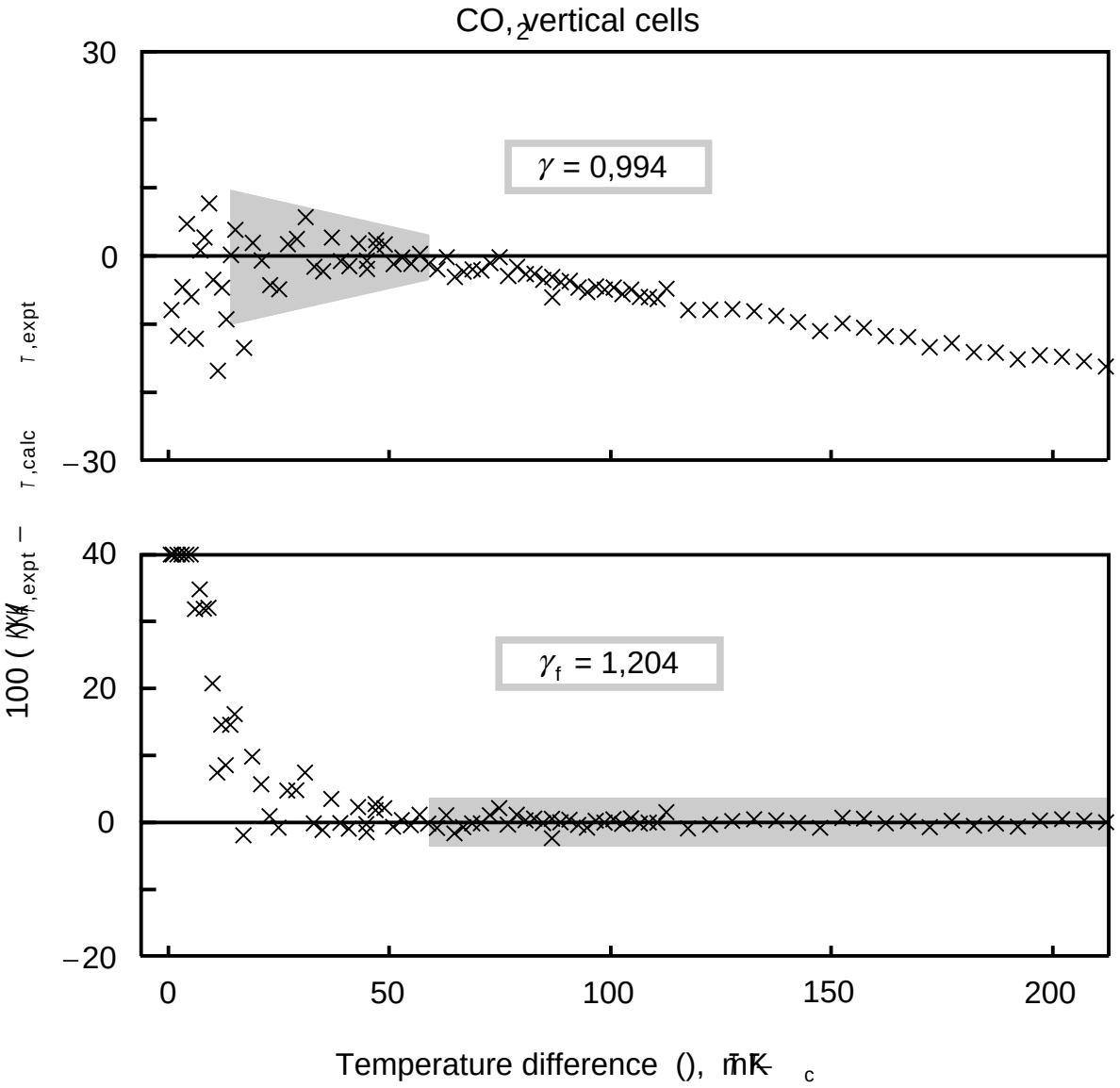
CO2, vertical cells
30
0
−30
γ = 0,994
40
20
0
−20
γf = 1,204
0
50
100
150
200
Temperature difference (), mK

Fig. 5